

## Synthesis and photopolymerization of novel, highly reactive phosphonated-urea-methacrylates for dental materials



Ayşe Altın<sup>a</sup>, Burcin Akgün<sup>a</sup>, Özlem Büyükgümüş<sup>a</sup>, Zeynep Saraylı Bilgici<sup>a</sup>, Sesil Agopcan<sup>a</sup>, Didar Asik<sup>b</sup>, Havva Yagci Acar<sup>c</sup>, Duygu Avcı<sup>a,\*</sup>

<sup>a</sup> Department of Chemistry, Bogazici University, 34342 Bebek, Istanbul, Turkey

<sup>b</sup> Department of Molecular Biology and Genetics, Koc University, Rumelifeneri Yolu, Sariyer, Istanbul, Turkey

<sup>c</sup> Department of Chemistry, Koc University, Rumelifeneri Yolu, Sariyer, Istanbul, Turkey

### ARTICLE INFO

#### Article history:

Received 23 January 2013

Received in revised form 30 June 2013

Accepted 2 July 2013

Available online 16 July 2013

#### Keywords:

Synthesis

Photopolymerization

Dental composites

Reactive diluents

Phosphonates

### ABSTRACT

An urea methacrylate (**1**) and two phosphonated methacrylates (**2–3**) were synthesized from 2-isocyanatoethyl methacrylate (IEM) and benzyl amine (**1**), diethyl aminomethylphosphonate (**2**) and diethyl amino(phenyl)methylphosphonate (**3**). Their photopolymerization rates are notably higher than commercial monomers, despite the presence of only one double bond. Their polymerization rates follow the order **1** ~ **2** > **3** ~ triethylene glycol dimethacrylate (TEGDMA) > 2-hydroxyethyl methacrylate (HEMA). A tendency toward high crosslinking density during thermal bulk polymerizations, low oxygen sensitivity and high conversions with benzophenone during photopolymerization indicated the importance of hydrogen abstraction/chain transfer reactions. It was found that the addition of the monomers to HEMA significantly increased its polymerization rate, proving their utility as replacements for TEGDMA as reactive diluents for 2,2-bis[4-(2-hydroxy-3-methacryloyloxy propoxy) phenyl] propane (Bis-GMA). Copolymer systems containing **2** and **3** showed improved  $T_g$  values compared to Bis-GMA/TEGDMA systems.

© 2013 Elsevier Ltd. All rights reserved.

### 1. Introduction

Acrylates and methacrylates are the most commonly used monomers in photoinitiated polymerizations due to their high reactivities and the excellent properties (especially optical and mechanical) of their resultant polymers, which find use as dental restorative materials, biomaterials, coatings, adhesives and in photolithography [1–5]. Extensive research has been performed to investigate the relationship between the structure of potential monomers and their reactivity to enhance the polymerization process and final materials [6–17].

Among the hydrogen bonding monomers investigated by Janzen and Berchtold, monomers containing urea were found to be the most reactive [14,15]. For example, the photopolymerization rate of ethyl urea ethyl acrylate ( $25.2 \text{ mol ls}^{-1}$ ) was higher than that of ethyl O-urethane-N-ethyl acrylate ( $16.1 \text{ mol ls}^{-1}$ ) and ethyl ester ethyl acrylate ( $4.4 \text{ mol ls}^{-1}$ ) [14]. Benzyl urea ethyl methacrylate was found to be the most reactive of any of the urethane, carbonate, cyclic carbonate, ester, or hydroxyl monomers studied by Berchtold et al. [15] The high reactivities were explained by a hydrogen bonding-induced pre-organization

that brings double bonds close to each other, enhancing propagation. Alternatively, a reduction in termination rate may also be involved in, or be the sole cause of, the observed reactivity.

The monomer 2,2-bis[4-(2-hydroxy-3-methacryloxyprop-1-oxy)phenyl]propane (Bis-GMA) is the most commonly used precursor for dental composite materials due to its high mechanical strength, low volatility and low polymerization shrinkage [3,18,19]. However, its high viscosity requires dilution with a low viscosity monomer, such as triethylene glycol dimethacrylate (TEGDMA), to improve both the double bond conversion and its ease of handling. Although the double bond conversion is increased by the addition of TEGDMA, increased volume shrinkage and shrinkage-associated stress decreases the bond strength between the tooth tissue and composite, initiating bacterial leakage and decreasing the lifetime of the dental composite. When Bis-GMA is copolymerized with TEGDMA, a final conversion of 50–75% is obtained depending on the monomer composition and photopolymerization conditions. These low conversions are due to the formation of a highly crosslinked polymer in the early stages of polymerization that restricts mobility within the system, decreasing both the propagation and termination rates. Therefore, in recent years, various highly reactive mono-(meth)acrylates have been investigated as alternatives to TEGDMA. With the use of such

\* Corresponding author. Tel.: +90 2123596816; fax: +90 2122872467.

E-mail address: [avcid@boun.edu.tr](mailto:avcid@boun.edu.tr) (D. Avcı).

monomers, similar levels of crosslinking density are attained at much higher conversions because these reactive monomer are less prone to affect crosslinking than TEGDMA.

We propose that urea-containing monomers may be suitable for this purpose. To test this hypothesis, we designed two new urea-containing monomers functionalized with phosphonate groups for improved biocompatibility and binding properties. A previously reported [15], structurally similar monomer was also investigated to test the correlation between the monomer structure and photopolymerization reactivity. Both homopolymerizations and copolymerizations with commercial dental monomers were investigated.

## 2. Experimental

### 2.1. Materials

Diethyl amino(phenyl)methylphosphonate and diethyl aminomethylphosphonate were prepared according to literature procedures [20,21]. Chloroform was dried over activated molecular sieves (4 Å<sup>0</sup>). Diethyl phosphite, 2-isocyanatoethyl methacrylate (IEM), Al(OTf)<sub>3</sub>, benzaldehyde, diethyl phthalimidomethylphosphonate, hydrazine hydrate, 2-hydroxyethyl methacrylate (HEMA), triethylene glycol dimethacrylate (TEGDMA), hexyl acrylate (HA), 2,2-bis[4-(2-hydroxy-3-methacryloyloxypropyloxy) phenyl] propane (Bis-GMA), 2,2'-azobis(isobutyronitrile) (AIBN), 2,2'-dimethoxy-2-phenyl acetophenone (DMPA), benzophenone (BP) and all other reagents and solvents were obtained from Aldrich Chemical Co. and used as received.

### 2.2. Characterization

<sup>1</sup>H, <sup>13</sup>C and <sup>31</sup>P NMR spectra were obtained on Varian Gemini (400 MHz) spectrometer. IR spectra were obtained on a Nicolet 6700 FTIR spectrometer. Elemental analyses were obtained on a Thermo Electron SpA FlashEA 1112 elemental analyzer (CHNS separation column, PTFE; 2 m; 6 × 5 mm). Photopolymerizations were performed using a TA Instruments Q100 differential photocalorimeter (DPC). Dynamic mechanical analysis (DMA) was performed on a Perkin Elmer Pyris Diamond DMA.

### 2.3. Synthesis of monomers

#### 2.3.1. General procedure for the synthesis of monomers 1–3

To an ice-cold solution of the desired amine (2.8 mmol) in 10.2 mL of dry chloroform under a stream of nitrogen, 2-isocyanatoethyl methacrylate (2.9 mmol, 0.41 mL) was added dropwise. The solution was stirred at room temperature overnight under nitrogen and then extracted with 1 wt% NaOH (3 × 42 mL), 1 wt% HCl (3 × 42 mL), and brine (3 × 42 mL). The organic layer was dried over anhydrous sodium sulfate, filtered and evaporated under reduced pressure to leave the crude product.

**2.3.1.1. Monomer 1.** The crude product was recrystallized from diethyl ether and dried under vacuum. The pure product was obtained as a white solid in 75% yield (mp = 70 °C).

<sup>1</sup>H NMR (400 MHz, CDCl<sub>3</sub>, δ): 1.82 (s, 3H, CH<sub>3</sub>), 3.33 (t, 2H, OCH<sub>2</sub>CH<sub>2</sub>), 4.07 (t, 2H, OCH<sub>2</sub>CH<sub>2</sub>), 4.21 (s, 2H, CH<sub>2</sub>–Ar), 5.12, 5.26 (bs, 2H, NH), 5.46, 5.98 (s, 2H, C=CH<sub>2</sub>), and 7.16–7.24 (m, 5H, Ar–H).

<sup>13</sup>C NMR (400 Mz, CDCl<sub>3</sub>, δ): 18.34 (CH<sub>3</sub>), 39.58 (OCH<sub>2</sub>CH<sub>2</sub>), 44.47 (NH–CH<sub>2</sub>), 64.08 (OCH<sub>2</sub>CH<sub>2</sub>), 125.96 (CH<sub>2</sub>=C), 135.96 (CH<sub>2</sub>=C), 127.30, 127.36, 128.60, 139.10 (Ar–C), 158.21 (HN–C=O), and 167.53 (O–C=O) ppm.

FTIR (ATR): 3321 (N–H), 3060, 3062 (Ar–H), 2960, 2928, 2890 (C–H), 1711 (C=O), 1628 (C=C), and 1587 (N–H) cm<sup>-1</sup>.

**2.3.1.2. Monomer 2.** The pure product was obtained as a colorless viscous liquid in 77% yield.

<sup>1</sup>H NMR (400 MHz, CDCl<sub>3</sub>, δ): 1.25 (t, 6H, OCH<sub>2</sub>CH<sub>3</sub>), 1.87 (s, 3H, CH<sub>3</sub>), 3.43 (t, 2H, OCH<sub>2</sub>CH<sub>2</sub>), 3.60 (m, 2H, CH<sub>2</sub>–P), 4.02 (m, 4H, OCH<sub>2</sub>CH<sub>3</sub>), 4.13 (t, 2H, OCH<sub>2</sub>CH<sub>2</sub>), 5.80, 6.43 (s, 2H, C=CH<sub>2</sub>), 6.05, 6.25 (bs, 2H, NH) ppm.

<sup>13</sup>C NMR (400 MHz, CDCl<sub>3</sub>, δ): 15.36 (OCH<sub>2</sub>CH<sub>3</sub>), 17.17 (CH<sub>3</sub>), 33.21, 34.95 (CH<sub>2</sub>–P), 38.15 (OCH<sub>2</sub>CH<sub>2</sub>), 61.60 (OCH<sub>2</sub>CH<sub>3</sub>), 63.31 (OCH<sub>2</sub>CH<sub>2</sub>), 124.76 (CH<sub>2</sub>=C), 135.14 (CH<sub>2</sub>=C), 157.59 (HN–C=O), and 166.28 (O–C=O) ppm.

FTIR (ATR): 3349 (N–H), 2983, 2929, 2901 (C–H), 1716, 1686 (C=O), 1644 (C=C), 1561 (N–H), 1215 (P=O), 1019, 948 (P–O–Et) cm<sup>-1</sup>.

<sup>31</sup>P NMR (CDCl<sub>3</sub>): 24.44 ppm.

**2.3.1.3. Monomer 3.** The crude product was recrystallized from diethyl ether and washed with hexane. The pure product was obtained as a white solid in 70% yield (mp = 72 °C).

<sup>1</sup>H NMR (400 MHz, CDCl<sub>3</sub>, δ): 1.01, 1.29 (t, 6H, OCH<sub>2</sub>CH<sub>3</sub>), 1.78 (s, 3H, CH<sub>3</sub>), 3.35 (m, 2H, OCH<sub>2</sub>CH<sub>2</sub>), 3.59, 3.77, 4.01 (m and t, 4H, OCH<sub>2</sub>CH<sub>3</sub>), 4.15 (m, 2H, OCH<sub>2</sub>CH<sub>2</sub>), 5.36, 5.91 (s, 2H, C=CH<sub>2</sub>), 5.41 (dd, 1H, CH–P), 5.99 and 7.09 (t and dd, 2H, NH), 7.20–7.41 (m, 5H, Ar–H) ppm.

<sup>13</sup>C NMR (400 MHz, CDCl<sub>3</sub>, δ): 16.16 (OCH<sub>2</sub>CH<sub>3</sub>), 18.05 (CH<sub>3</sub>), 38.73 (OCH<sub>2</sub>CH<sub>2</sub>), 49.87, 51.51 (CH–P), 63.18 (OCH<sub>2</sub>CH<sub>3</sub>), 64.01 (OCH<sub>2</sub>CH<sub>2</sub>), 125.44 (CH<sub>2</sub>=C), 136.03 (CH<sub>2</sub>=C), 127.81, 127.99, 128.34, 135.96 (Ar–C), 157.77 (HN–C=O), and 167.13 (O–C=O) ppm.

FTIR (ATR): 3379, 3317 (N–H), 3060, 3032 (Ar–H), 2987, 2929, 2907 (C–H), 1722, 1684 (C=O), 1638 (C=C), 1545 (N–H), 1216 (P=O), 1014, 980 (P–O–Et) cm<sup>-1</sup>.

<sup>31</sup>P NMR (CDCl<sub>3</sub>): 23.22 ppm.

ELEM. ANAL., Calcd. for C<sub>18</sub>H<sub>27</sub>N<sub>2</sub>O<sub>6</sub>P: C, 54.27%; H, 6.83%; N, 7.03%; O, 24.10%; P, 7.77%. Found: C, 54.54%; H, 7.31%; N, 7.31%.

### 2.4. Photopolymerization

Photopolymerizations were conducted using a DSC equipped with a mercury arc lamp. The samples (3–4 mg) containing 2.0 mol% initiator were irradiated for 10 min at either 40 °C or 72 °C with an incident light intensity of 20 mW/cm<sup>2</sup> and a nitrogen flow of 20 mL min<sup>-1</sup>. Polymerization rates were calculated using the following formula:

$$\text{Rate} = \frac{(Q/s)M}{n\Delta H_p m}$$

where Q/s is the heat flow per second, M the molar mass of the monomer, n the number of double bonds per monomer molecule, ΔH<sub>p</sub> the heat released per mole of double bonds reacted, and m is the mass of monomer in the sample. The value used for the ΔH<sub>p</sub> of a methacrylate double bond was 13.12 kcal/mol [22].

### 2.5. Calculation of dipole moments

Boltzmann-averaged dipole moments were calculated with PM3 for all the monomers. In this procedure, all possible rotations around single bonds were considered for a given acrylate to generate all the conformations corresponding to stationary points. Minimization, followed by the calculation of the Boltzmann-averaged dipole moments for all the conformations, was carried out with PM3 in the Spartan '06 program [23]. The unique structures were

sorted in order of increasing energy. The dipole moments of the first 100 conformers are Boltzmann averaged at 298.15 K according to the following formula:

$$\langle \mu_{\text{calc}} \rangle = \sum_j D_j \frac{e^{\Delta H_j/RT}}{\sum_i e^{\Delta H_i/RT}} = \sum_j D_j p_j$$

where  $D_j$  is the dipole moment of conformation  $j$ ,  $\Delta H_j$  the heat of formation of conformation  $j$ ,  $T$  the absolute temperature,  $R$  the Boltzmann constant, and  $p_j$  is the probability of finding the monomer in conformation  $j$  at temperature  $T$  [14].

### 2.6. Interactions with hydroxyapatite

HAP particles (0.2 g) were dispersed in 1.00 g of a monomer/EtOH/H<sub>2</sub>O (15:45:40 wt%) solution under stirring. After 24 h, the HAP particles were separated by centrifugation, and the material remaining after evaporation of the solvent was investigated using FT-IR.

### 2.7. Cytotoxicity testing

Mouse fibroblast cells (NIH-3T3) were cultured at a density of  $2 \times 10^4$  cells/well in 96-well plates containing DMEM culture media supplemented with 10% L-glutamine, 10% fetal bovine serum and 1% penicillin–streptomycin. Trypsin–EDTA was used for cell detachment. Cells were incubated at 37 °C under 5% CO<sub>2</sub> for 24 h.

The cytotoxicities of the synthesized monomers and Bis-GMA on NIH-3T3 cells were determined using MTT cell viability assays. Cells were incubated with monomers **1–3** and Bis-GMA at doses between 10–100 μM for 24 h at 37 °C under a 5% CO<sub>2</sub> humidified atmosphere. After this time, the medium was aspirated and the cells were incubated in fresh medium containing MTT for 4 h. The formazan product that formed due to mitochondrial activity was dissolved with DMSO:EtOH (1:1), and its absorbance was measured on an ELx800 Biotek Elisa reader at 600 nm. The viability of cells incubated with chemicals was expressed as a percentage of the viability of control cells. The statistical significance of all the results was analyzed by one-way ANOVA with Tukey's multiple comparison test within the Graph Pad Prism 5 software package from GraphPad Software, Inc., USA. Each experiment was repeated four times.

The tested monomers and Bis-GMA were dissolved in dimethyl sulfoxide (DMSO) hybri-max. The solutions were diluted with distilled water and filtered with a 0.20 μm sterile single-use syringe filter. The maximum amount of DMSO in each well was set to 0.25% of the medium (200 μL) as this amount of DMSO has been reported to be non-toxic [24]. As a control, cells were incubated with 0.25% DMSO and the cell viability was compared with cells treated only with DMEM.

### 2.8. Dynamic mechanical analysis (DMA)

Samples studied by DMA were photopolymerized in a Teflon mold (10 × 7 × 3 mm) with 10 mW/cm<sup>2</sup> of UV radiation for 15 min at room temperature. The polymerized samples were post-cured at 80 °C for 2 h. Analyses were performed over a temperature range of 10–200 °C with a ramping rate of 5 °C/min in extension mode. The loss and storage moduli, as well as the loss tangent, were recorded as a function of temperature. The glass transition temperature ( $T_g$ ) was taken to be the maximum of the loss tangent versus temperature curve.

### 2.9. Water sorption and solubility

Water sorption and water solubility were measured according to ISO 4049 [25]. Three samples, which were 15 ± 0.3 mm in diam-

eter and 1.5 ± 0.4 mm in thickness, were used. The compositions and photopolymerization conditions of the studied materials were the same as those used for the samples studied by DMA. The samples were dried to a constant weight in air at 37 °C with the weight recorded as  $m_1$ . The samples were immersed in water and maintained at 37 °C for 7 days. The samples were then removed, blotted to remove surface water, dried in air (15 s), and weighed. This measurement was recorded as  $m_2$ . Both samples were then stored in an oven containing anhydrous calcium chloride at 37 °C until a new constant weight was reached ( $m_3$ ). The volumes of the samples ( $V$ ) were also measured.

The water sorption ( $W_{\text{sp}}$ ) and solubility ( $W_{\text{st}}$ ) were calculated using the following equations:

$$W_{\text{sp}} = \frac{m_2 - m_1}{V}$$

$$W_{\text{st}} = \frac{m_3 - m_1}{V}$$

## 3. Results and discussion

### 3.1. Monomer synthesis

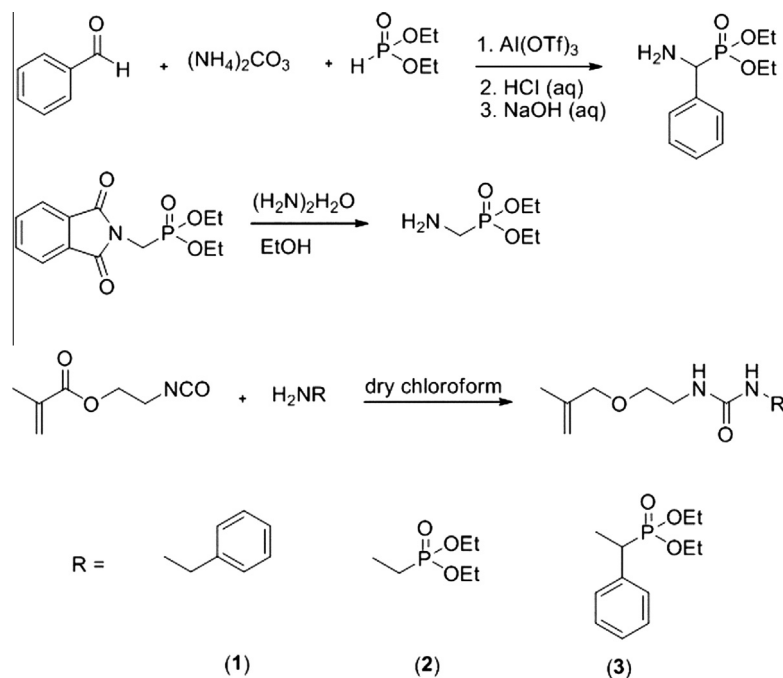
Three primary amines were used as starting materials for the monomers synthesized in this work. The first amine (benzyl amine) was commercially available. The second (diethyl aminomethylphosphonate) was synthesized from the reaction of diethyl phthalimidomethylphosphonate with hydrazine hydrate in ethanol [21]. The third amine (diethyl amino(phenyl)methylphosphonate) was synthesized in a solvent-free one-pot reaction of benzaldehyde, ammonium carbonate and diethyl phosphite in the presence of catalytic Al(OTf)<sub>3</sub> (Scheme 1) [20].

The monomers were synthesized in one-pot reactions of the amines with IEM at room temperature in dry chloroform for 12 h (Scheme 1). Monomers **1** and **3** were obtained as solids with melting points of 70 and 72 °C, respectively, while monomer **2** was a liquid. All yields were greater than 70%. The monomers were soluble in acetone, THF, chloroform, methanol and ether but were insoluble in water and hexane. They were characterized using a combination of <sup>1</sup>H, <sup>13</sup>C, <sup>31</sup>P NMR and FTIR spectroscopies.

The <sup>1</sup>H NMR spectrum of monomer **2** showed peaks characteristic of methyl protons at 1.25 and 1.87 ppm; methylene protons adjacent to nitrogen, phosphorus and oxygens at 3.43, 3.60, 4.02 and 4.13 ppm; and double-bond hydrogens at 5.80 and 6.43 ppm (Fig. 1). The NH protons were confirmed by the presence of two broad peaks at 6.05 and 6.25 ppm. Surprisingly, in the <sup>1</sup>H NMR spectrum of monomer **3**, we observed two sets of phosphonate ester ethyl peaks due to the different resonance forms of the amide linkage.

In the <sup>13</sup>C NMR spectrum of monomer **3**, the methine carbon attached to phosphorus is indicated by the presence of a doublet at approximately 50.7 ppm (Fig. 2). In the <sup>31</sup>P NMR spectra of monomers **2** and **3**, the presence of only one peak at approximately 23 ppm, a typical shift for phosphonates, confirmed the purity of the monomers (Fig. 2).

The FTIR spectra of each monomer showed stretching peaks indicative of the NH of the hydrogen bonded urea groups at approximately 3320–3378 cm<sup>-1</sup> (Fig. 3). Monomer **3** displayed two peaks due to the cis- and trans-isomers of the hydrogen-bonded urea groups. The presence of a single NH peak in monomers **1** and **2** is most likely due to the coincidental overlap of the two isomer peaks (monomer **2**) or the interconvertibility of the two conformations (monomer **1**). The free NH stretching vibration, which would appear as a shoulder at approximately 3400 cm<sup>-1</sup>, was not obvious. The stretching vibrations of ester carbonyl groups were found from 1711 (**1**) to 1722 (**3**) cm<sup>-1</sup>. The monomers showed peaks in the region typical for the C=O stretch of urea



**Scheme 1.** Synthesis of amines and monomers.

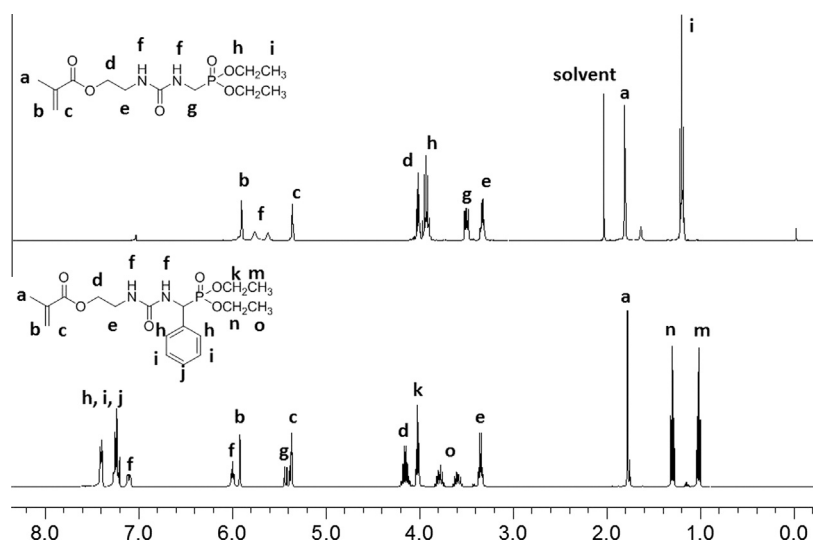


**Fig. 1.**  $^1\text{H}$  NMR spectra of monomers **2** and **3**.

groups ( $1627\text{--}1684\text{ cm}^{-1}$ ). The temperature dependence of the FTIR spectrum of one of the monomers (**3**) was also investigated. Fig. 3 shows the carbonyl stretching region of monomer **3** heated from  $40$  to  $200\text{ }^\circ\text{C}$ . The band at  $1722\text{ cm}^{-1}$  was assigned to stretching of the free ester carbonyl groups, while the band at  $1714\text{ cm}^{-1}$  was attributed to hydrogen-bonded ester carbonyl groups. As the temperature was increased from  $40$  to  $200\text{ }^\circ\text{C}$ , the peaks observed for the hydrogen-bonded ester carbonyl decreased from  $1714$  to  $1719\text{ cm}^{-1}$ . The free ester carbonyl stretching absorbance also shifted to  $1719\text{ cm}^{-1}$  when heated to  $90\text{ }^\circ\text{C}$ , likely due to melting, and it then remained constant up to  $200\text{ }^\circ\text{C}$ . The frequency of the hydrogen-bonded urea carbonyl band shifted from  $1684$  to  $1692\text{ cm}^{-1}$  at approximately  $80\text{ }^\circ\text{C}$ . These results implied that the both the ester and urea carbonyls participate in hydrogen bonding.

### 3.2. Interactions with hydroxyapatite

The interaction of monomers **2** and **3** with HAP, a material representative of dental tissues, was investigated by FTIR. Solutions composed of individual monomers and HAP showed significant decreases in intensity and broadening of a peak near  $1216\text{ cm}^{-1}$ , attributable to  $\text{P}=\text{O}$  stretching. These changes indicated the interaction of both monomers with HAP (see SM).

### 3.3. Cytotoxicity testing

According to the cytotoxicity results: (i) The use of DMSO in sample preparation had no toxic effect on NIH-3T3 cells, and (ii) Bis-GMA, monomers **1**, **2** and **3** had no significant toxicity on

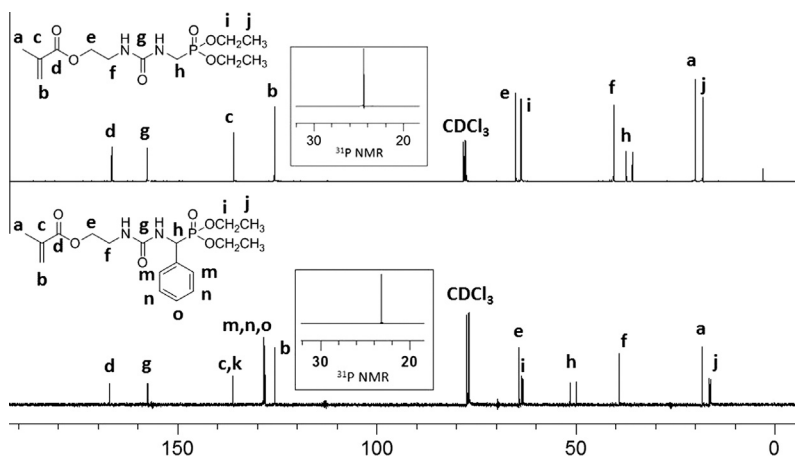


Fig. 2.  $^{13}\text{C}$  and  $^{31}\text{P}$  NMR spectra of monomers **2** and **3**.

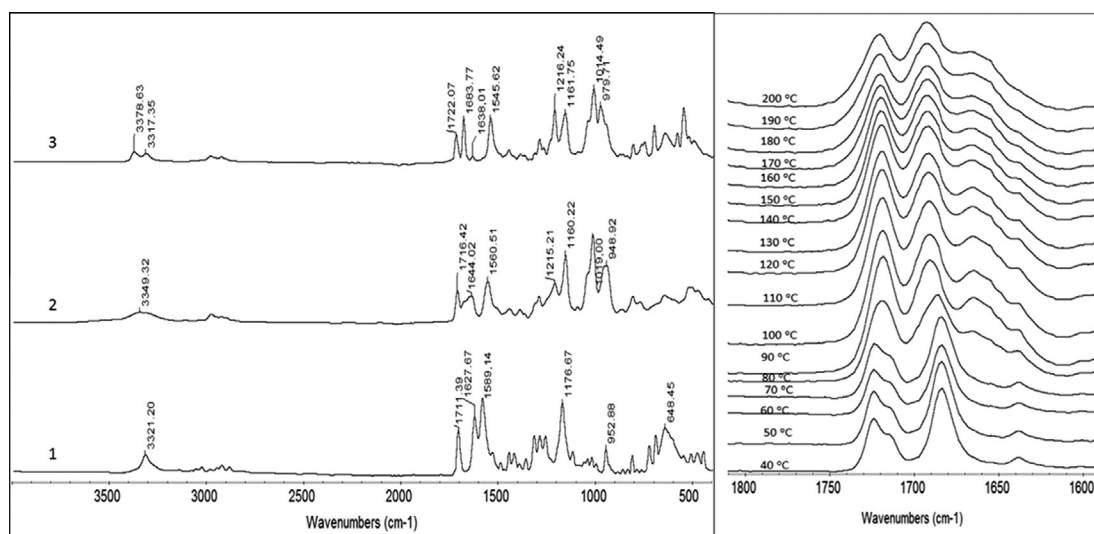


Fig. 3. FTIR spectra of monomers at room temperature and temperature dependence of the FTIR spectrum of monomer **3** in the carbonyl stretching region.

NIH-3T3 cells ( $P < 0.05$ ) at 10, 30, and 50  $\mu\text{M}$  doses. Significant toxicity was only detected at 100  $\mu\text{M}$  concentrations for monomers **2** and **3**. Monomer **2** was more toxic than monomer **3** (see SM).

#### 3.4. Photopolymerizations

Photopolymerizations of the synthesized methacrylates were investigated with photodifferential scanning calorimetry using DMPA (2 mol%) as a photoinitiator. However, because only monomer **2** was a liquid at room temperature (see Section 2), the three could only be compared at 72  $^{\circ}\text{C}$ . For comparison, two commercial monomers, TEGDMA and HEMA, were also polymerized under the same conditions.

Photopolymerization of the synthesized monomers started at a higher rate than HEMA and TEGDMA. After 5 s of polymerization, 53.7%, 54.1%, and 39.5% of the double bonds were reacted for monomers **1**, **2**, **3**, respectively, and only 16.3% and 4.5% for TEGDMA and HEMA. These values indicated that autoacceleration of the polymerization rate occurred earlier with the synthesized monomers than in the commercial materials. This behavior is typical for multifunctional (meth)acrylates. The maximum observed rates were in the following order: **1**  $\sim$  **2**  $>$  **3**  $\sim$  TEGDMA  $>$  HEMA (Fig. 4). To investigate the photopolymerization behavior of the synthesized monomers in more detail, their polymerization rates were also compared at 10% conversion and found to be 0.060,

0.064 and 0.084  $\text{s}^{-1}$  for monomers **1**, **2** and **3**, respectively. The initial rate of polymerization of monomer **3** is clearly higher than those of **1** and **2**. The lower maximum rate of polymerization of this monomer, compared to those of **1** and **2**, can be explained by early gelation, which decreases both the propagation and termination rates.

It is known that increased functionality of a particular monomer generally increases its polymerization rate but decreases its overall monomer conversion. Thus, TEGDMA would be expected to have a higher polymerization rate than monomers **1–3** and HEMA. However, the synthesized monomers react very rapidly despite having only one double bond. This can be attributed to hydrogen bonding, as will be discussed.

Overall polymer conversions were found to be similar (85–92%) for monomers **1**, **2** and TEGDMA. Although the maximum rate of polymerization of monomer **3** is similar to TEGDMA, and higher than HEMA, the conversion of **3** was found to be lower (65%) than either TEGDMA or HEMA. This result may be attributed to early autoacceleration and/or a high  $T_g$  of its polymer due to the rigid structures of both the monomer and polymer. In fact, the percent-conversions at the point of maximum rate were found to be 20.8%, 22.1% and 7.6% for monomers **1**, **2** and **3**, respectively.

All of the synthesized monomers have the capability of hydrogen bonding, an important rate enhancing factor, due to urea linkages. Hoyle et al. showed a direct relation between the degree of

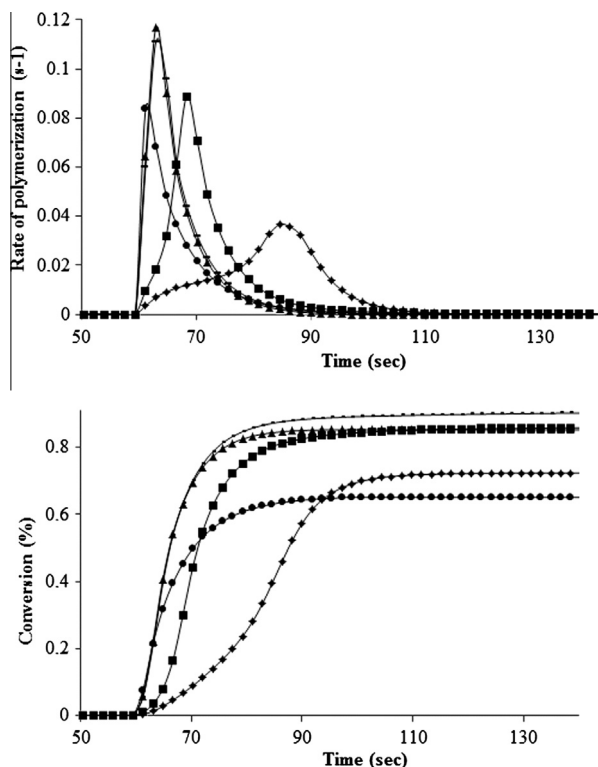


Fig. 4. Rate-time and conversion-time plots in the polymerizations of **1** (–), **2** (▲), and **3** (●), HEMA (◆) and TEGDMA (■) at 72 °C with 2 mol% DMPA.

hydrogen bonding and the rate of polymerization of hydroxyalkyl acrylates. Both the degree of hydrogen bonding and the polymerization rate were found to decrease with increasing temperature. Although no quantitative relationship was found between hydrogen bonding and the termination rate constants, the authors postulated that highly hydrogen-bonded systems behave as multifunctional monomers and have correspondingly low termination constants [16]. However, a similar claim for methacrylates is weaker [17].

The effect of temperature on the polymerization rate of the monomers synthesized in this work was of interest. The polymerization rate of monomer **2** at three different temperatures was measured using photo-DSC. In general, the rate increased with increasing temperature, with values of 0.08, 0.1 and 0.12 s<sup>-1</sup> at 40, 55 and 72 °C, respectively. However, we were unable to identify a clear trend, which may indicate that hydrogen bonding is not the only parameter affecting the reaction rate.

Thermal bulk polymerization of monomers **1–3** using 2 wt% AIBN at 65 °C yielded crosslinked polymers in 4–15 min, indicating the possible existence of hydrogen abstraction reactions. The labile hydrogens on methylene or methine next to phosphonate and/or phenyl groups are likely responsible for this behavior. To investigate this possibility, photopolymerizations of the monomers were investigated at 72 °C using BP (2 mol%) as a photoinitiator (Table 1). In the presence of BP, the photopolymerization rates were slower but the conversions were still very high. The maximum polymerization rate of monomer **2** was approximately three times lower with BP than with the same concentration of DMPA. However, the overall monomer conversions observed in both photoinitiator-systems were similar (~80%). When the photopolymerization of monomer **2** was conducted with BP (2 mol%) at 40 °C, the polymerization rate was six times lower than that achieved with DMPA; however, the conversion was still approximately 80%.

It is known that monomers with abstractable hydrogens in their structures may reduce the oxygen inhibition effect during

Table 1  
Photopolymerization results of monomers **1**, **2**, **3** and HA.

Monomer	Initiator	$R_{p,max}$ (s <sup>-1</sup> )	Conv. (%)
<b>1</b> <sup>a</sup>	DMPA	0.111	92
<b>2</b> <sup>a</sup>	DMPA	0.117	85
<b>3</b> <sup>a</sup>	DMPA	0.084	65
<b>1</b> <sup>a</sup>	BP	0.036	89
<b>2</b> <sup>a</sup>	BP	0.039	80
<b>2</b> <sup>b</sup>	BP	0.021	80
<b>3</b> <sup>a</sup>	BP	0.014	72
<b>1</b> <sup>a</sup>	–	0.008	73
<b>2</b> <sup>a</sup>	–	0.011	34
<b>2</b> <sup>b</sup>	–	0.007	20
<b>3</b> <sup>a</sup>	–	0.004	10
<b>2</b> <sup>b</sup>	DMPA	0.107	93
<b>2</b> <sup>b,c</sup>	DMPA	0.095	83
HA <sup>b</sup>	DMPA	0.037	69
HA <sup>b,c</sup>	DMPA	0.009	36

<sup>a</sup> 72 °C.

<sup>b</sup> 40 °C.

<sup>c</sup> In air.

free-radical photopolymerization [26]. Hydrogen abstraction generates a free-radical, which reduces oxygen to a peroxy radical, minimizing oxygen inhibition. Crosslinking, which decreases the diffusion rate of oxygen into samples from the atmosphere, may also have an effect on the degree of oxygen inhibition. To investigate the effect of abstractable hydrogen on the oxygen inhibition of free-radical polymerization, the polymerization rate of monomer **2** was measured in the presence and absence of oxygen (Table 1). Clearly, monomer **2** showed little oxygen inhibition in air (11% decrease in rate), whereas HA (76% decrease in air) was very sensitive to the presence of air. These findings support our proposed hydrogen abstraction/chain transfer mechanism.

As monomers **1–3** are very reactive, their use in an initiator-free polymerization environment was investigated. All three monomers showed some polymerization in the absence of initiator at 72 °C, although both rates and conversions suffered (Table 1). The results of the polymerization of monomer **2** at lower temperature (40 °C) suggested that self-initiation is, to some degree, temperature dependent.

The relationship between the polarity of monomers **1–3** and their polymerization reactivities was studied. The Boltzmann-averaged dipole moments for the minimum energy conformations of the monomers were calculated as 3.27, 4.47 and 4.32 Debye for **1**, **2** and **3**, respectively. No clear correlation between the dipole moment and reactivity was observed. The influences of hydrogen bonding and hydrogen abstraction dominate any effect that the dipole moment may have.

### 3.5. Copolymerizations with dental monomers

To test the use these monomers as both crosslinkers in dental adhesives and as reactive diluents in filling composites, we investigated their copolymerization with HEMA and Bis-GMA, which are important monomers in dental applications. Fig. 5 shows the results of the copolymerizations of monomers **1–3** with HEMA at 40 °C in the presence of DMPA. The addition of 10 mol% of monomers **1–3** to HEMA increased its polymerization rate significantly, presumably due to the enhanced hydrogen bonding provided by the urea groups. Surprisingly, the effect of monomer **3** was the strongest of the three. An explanation for this phenomenon lies with the large steric bulk of monomer **3**. While the initial polymerization of monomer **3** is faster than monomers **1** and **2** (Fig. 5), its prolonged reactivity is hindered by the presence of two bulky groups (benzyl and phosphonate). The increased mobility of HEMA

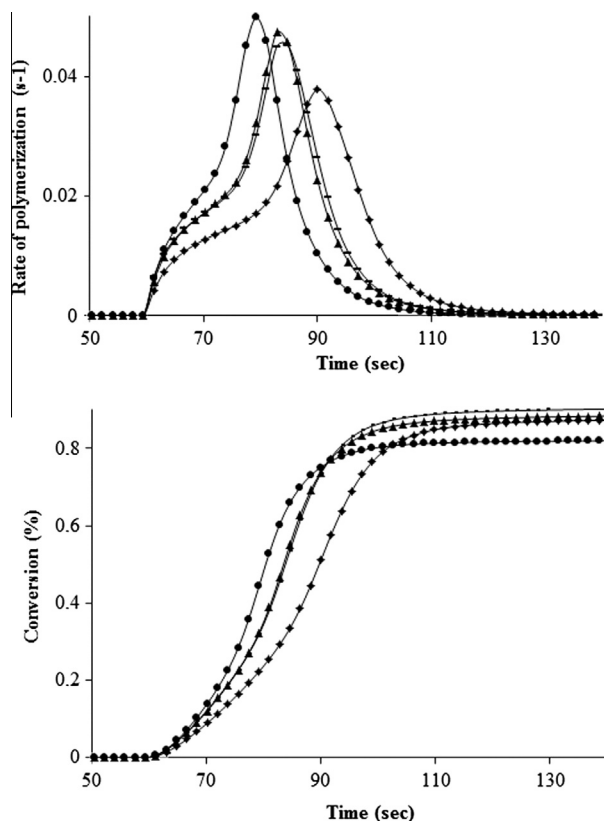


Fig. 5. Rate-time and conversion-time plots of HEMA (♦) and its copolymers with 10 mol% of **1** (-), **2** (▲) and **3** (●) at 40 °C with 2 mol% DMPA.

may alleviate this hindrance. Unfortunately, this steric effect decreased the overall conversion of HEMA.

In the experimental conditions employed, the maximum rate and final conversion obtained for the Bis-GMA/TEGDMA system (50:50 mol%) were  $0.084 \text{ s}^{-1}$  and 72% at 40 °C, respectively (Fig. 6). Although monomer **2** was found to be more reactive than Bis-GMA and TEGDMA, the replacement of TEGDMA with this monomer gave a maximum polymerization rate and monomer conversion of  $0.074 \text{ s}^{-1}$  and 74%, respectively. These unexpectedly low values can be explained by the higher viscosity of monomer **2** ( $0.013 \text{ Pa s}$ ), imparted by hydrogen bonding, compared to that of TEGDMA ( $0.009 \text{ Pa s}$ ). The increased viscosity causes a decrease in the mobilities of reactive species in the system and the resulting lower polymerization rate.

An alternative explanation of this unexpected result revolves around the glass transition temperature ( $T_g$ ) of monomer **2**. The  $T_g$  value is a measure of monomer flexibility and mobility in the polymerizing system. A correlation between monomer conversion and monomer  $T_g$  values has been reported [27]. Bis-GMA, which displays strong hydrogen bonding, has a very high  $T_g$  value ( $-6.6$  °C), while the very flexible monomer TEGDMA had a value of  $-81.7$  °C. Their 50:50 mol% mixture has a  $T_g$  value of  $-51.0$  °C and shows more complete conversion (72%) than neat Bis-GMA (64%). The  $T_g$  value of the Bis-GMA/monomer **2** (50:50 mol%) mixture was found to be higher ( $-28$  °C) than that of a similar Bis-GMA/TEGDMA (50:50 mol%) mixture ( $-51.0$  °C) (Table 2), which is consistent with the lower observed conversion value of the Bis-GMA/monomer **2** (50:50 mol%) mixture. The  $T_g$  value of monomer **2** ( $-51.4$  °C) was found to be considerably greater than that of TEGDMA ( $-81.7$  °C).

TEGDMA could not be totally replaced with monomers **1** and **3**, as they are solids at room temperature and do not form clear

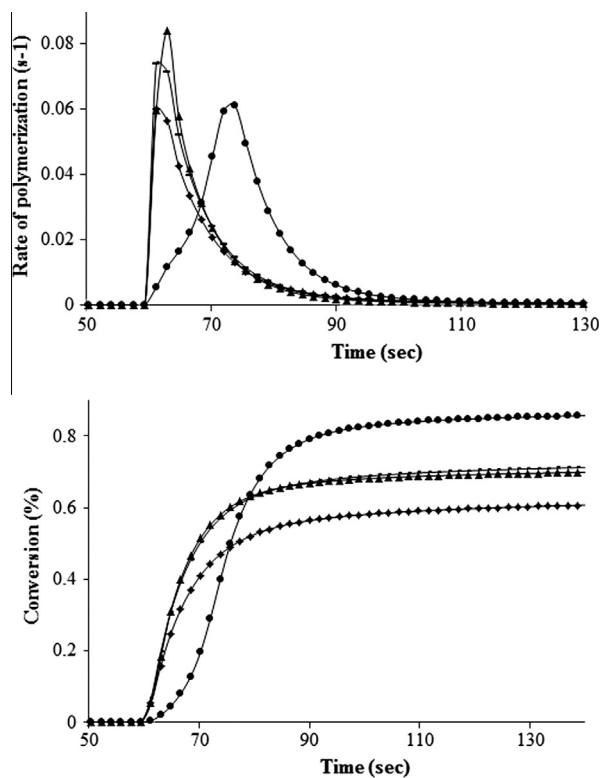


Fig. 6. Rate-time and conversion-time plots in the polymerizations of 2-Bis-GMA (50:50 mol%): (-), TEGDMA/Bis-GMA (50:50 mol%): (▲), TEGDMA: (●) and Bis-GMA: (♦) at 40 °C with 2 mol% DMPA.

Table 2

Photopolymerization results of monomers **1**, **2** and **3** with Bis-GMA and TEGDMA at 40 °C and glass transition temperatures of monomeric states ( $T_g$ ).

Bis-GMA (mol%)	TEGDMA (mol%)	Monomers ( <b>1</b> , <b>2</b> , <b>3</b> ) (mol%)	$R_p$ ( $\text{s}^{-1}$ )	Conversion (%)	$T_g$ (°C)
100	-	-	0.060	64	-6.6 [28]
-	100	-	0.061	87	-81.7 [28]
50	50	-	0.084	72	-51.0
80	20	-	0.074	65	-
-	-	100 ( <b>1</b> )	0.073	84	-
80	10	10 ( <b>1</b> )	0.079	72	-
50	40	10 ( <b>1</b> )	0.078	71	-
50	20	30 ( <b>1</b> )	0.093	70	-
-	-	100 ( <b>2</b> )	0.073	84	-51.4
50	-	50 ( <b>2</b> )	0.074	74	-28.0
50	20	30 ( <b>2</b> )	0.078	75	-
50	20	30 ( <b>3</b> )	0.077	66	-

solutions with BisGMA. Consequently, TEGDMA was only partially substituted with various concentrations of one or the other of these monomers (Table 2). The results indicated that either one of the monomers may effectively replace TEGDMA, either totally or partially. The rates/conversions did not significantly differ in systems with or without our monomers, although one formulation displayed a somewhat higher rate.

The DMA results indicated that copolymer systems containing phosphonated urea-methacrylates (**2** and **3**) showed narrower, more well-defined glass transition peaks than Bis-GMA/TEGDMA polymers (see SM). Broad glass transition peaks are indicators of heterogeneity in polymer systems [29]. Therefore, the formulations

**Table 3**  
Tan  $\delta$ ,  $T_g$ , water sorption and solubility results.

	Bis-GMA/TEGDMA (50/50 mol%)	Bis-GMA/TEGDMA (70/30 mol%)	Bis-GMA/TEGDMA/2 (50/20/30 mol%)	Bis-GMA/TEGDMA/3 (50/20/30 mol%)
Tan $\delta$	0.167 0.203	0.258 0.225	0.294	0.378
$T_g$ (°C)	95 150	90 143	111	104
Water sorption ( $\mu\text{g}/\text{mm}^3$ )	28.9 (1.6)	28.3 (3.1)	37.8 (2.2)	33.5 (2.9)
Solubility ( $\mu\text{g}/\text{mm}^3$ )	11.4 (0.6)	18.0 (3.7)	12.0 (3.7)	13.4 (3.5)

containing phosphonated urea-methacrylates result in less heterogeneous polymers, which are prone to less softening at temperatures below the  $T_g$ . The  $T_g$  values of copolymers containing **2** and **3** were 104 and 114 °C, noticeably higher than those of the Bis-GMA/TEGDMA (70:30 and 50:50 mol%) systems (90 and 95 °C) (Table 3). A higher  $T_g$  value is indicative of higher crosslinking and thermal stability.

Water sorption and water solubility data of the copolymer systems are presented in Table 3. According to the ISO 9000 standard, the maximum values of water sorption and solubility for dental resins are 50  $\mu\text{g}/\text{mm}^3$  and 5  $\mu\text{g}/\text{mm}^3$ , respectively [25]. The copolymer systems containing phosphonated urea-methacrylates showed water sorption characteristics similar to the Bis-GMA/TEGDMA systems.

#### 4. Conclusion

Two novel phosphonated urea-monomethacrylates (**2** and **3**) and one other urea-methacrylate (**1**) were synthesized and evaluated for possible applications in dental composites and adhesives. The homo- and copolymerization behaviors of the synthesized monomers with HEMA and Bis-GMA were investigated using photodifferential scanning calorimetry. The reactivities of these monovinyl methacrylates were found to surpass the reactivity of TEGDMA. The significantly enhanced polymerization rates and conversions of these monomers were explained by a combination of hydrogen abstraction/chain transfer reactions due to labile hydrogens and hydrogen bonding imparted by the urea linkages. The low oxygen sensitivity of one of the monomers and the polymerizability with benzophenone are consistent with crosslinking during thermal polymerization as a result of hydrogen abstraction/chain transfer reactions. The copolymerization of monomers **1–3** with HEMA resulted in improvements in the rate of HEMA polymerization and indicated their potential as biocompatible crosslinkers. Copolymerizability with Bis-GMA showed the capacity of monomers **1–3** to be used as reactive diluents with Bis-GMA replacing, either totally or partially, the conventionally used TEGDMA diluent. Utilizing phosphonated urea methacrylates (**2** and **3**) as reactive diluents resulted in improved glass transition temperatures.

#### Acknowledgement

Financial support by Bogazici University Research Fund (6728) is gratefully acknowledged.

#### Appendix A. Supplementary material

Supplementary data associated with this article can be found, in the online version, at <http://dx.doi.org/10.1016/j.reactfunctpolym.2013.07.006>.

#### References

- [1] J.G. Kloosterboer, Adv. Polym. Sci. 84 (1988) 1–61.
- [2] C. Decker, Prog. Polym. Sci. 21 (1996) 593–650.
- [3] K.S. Anseth, S.M. Newman, C.N. Bowman, Adv. Polym. Sci. 122 (1995) 177–217.
- [4] E. Andrzejewska, Prog. Polym. Sci. 26 (2001) 605–665.
- [5] N.M. Paul, S.J. Bader, S.R. Schrickler, J.R. Parquette, React. Funct. Polym. 66 (2006) 1684–1695.
- [6] K. Moussa, C. Decker, J. Polym. Sci. Part A: Polym. Chem. 31 (1993) 2197–2203.
- [7] H. Kilambi, S.K. Reddy, L. Schneidewind, J.W. Stansbury, C.N. Bowman, J. Polym. Sci. Part A: Polym. Chem. 47 (2009) 4859–4870.
- [8] H. Lu, J.W. Stansbury, J. Nie, K.A. Berchtold, C.N. Bowman, Biomaterials 26 (2005) 1329–1336.
- [9] H. Kilambi, E.R. Beckel, K.A. Berchtold, J.W. Stansbury, C.N. Bowman, Polymer 46 (2005) 4735–4742.
- [10] E.R. Beckel, J.W. Stansbury, C.N. Bowman, Macromolecules 38 (2005) 9474–9481.
- [11] E.R. Beckel, J. Nie, J.W. Stansbury, C.N. Bowman, Macromolecules 37 (2004) 4062–4069.
- [12] K.A. Berchtold, J. Nie, J.W. Stansbury, C.N. Bowman, Macromolecules 41 (2008) 9035–9043.
- [13] E. Andrzejewska, M. Andrzejewski, J. Polym. Sci. Part A: Polym. Chem. 36 (1998) 665–673.
- [14] J.F.G.A. Jansen, A.A. Dias, M. Dorsch, B. Coussens, Macromolecules 36 (2003) 3861–3873.
- [15] K.A. Berchtold, J. Nie, J.W. Stansbury, B. Hacıoglu, E.R. Beckel, C.N. Bowman, Macromolecules 37 (2004) 3165–3179.
- [16] T.Y. Lee, T.M. Roper, E.S. Jönsson, C.A. Guymon, C.E. Hoyle, Macromolecules 37 (2004) 3659–3665.
- [17] H. Zhou, Q. Li, T.Y. Lee, C.A. Guymon, E.S. Jönsson, C.E. Hoyle, Macromolecules 39 (2006) 8269–8273.
- [18] N. Moszner, U. Salz, Prog. Polym. Sci. 26 (2001) 535–576.
- [19] M. Szaloki, J. Gall, K. Bukovinszki, J. Borbely, C. Hegedus, React. Funct. Polym. 73 (2013) 465–473.
- [20] S. Sobhani, Z. Tashrif, Synth. Commun. 39 (2009) 120–131.
- [21] P. Bakó, T. Novák, K. Ludányi, B. Pete, L. Töke, G. Keglevich, Tetrahedron-Asymmetry 10 (1999) 2373–2380.
- [22] J. Brandrup, E.H. Immergut, Polymer Handbook, Wiley-Interscience, New York, 1975.
- [23] SPARTAN version 4.0; Wavefunction, Inc.; 18401 Von Karman Ave., #370, Irvine, CA 92715 USA. ©1995 Wavefunction, Inc.
- [24] Y. Issa, D.C. Watts, P.A. Brunton, C.M. Waters, A.J. Duxbury, Dent. Mater. 20 (2004) 12–20.
- [25] M. Podgorski, Dent. Mater. 28 (2012) 398–409.
- [26] T.Y. Lee, C.A. Guymon, E.S. Jönsson, C.E. Hoyle, Polymer 45 (2004) 6155–6162.
- [27] I. Sideridou, V. Tserki, G. Papanastasiou, Biomaterials 23 (2002) 1819–1829.
- [28] S.G. Pereira, R. Osorio, M. Toledano, T.G. Nunes, Dent. Mater. 21 (2005) 823–830.
- [29] H. Kilambi, N.B. Cramer, L.H. Schneidewind, P. Shah, J.W. Stansbury, C.N. Bowman, Dent. Mater. 25 (2009) 33–38.